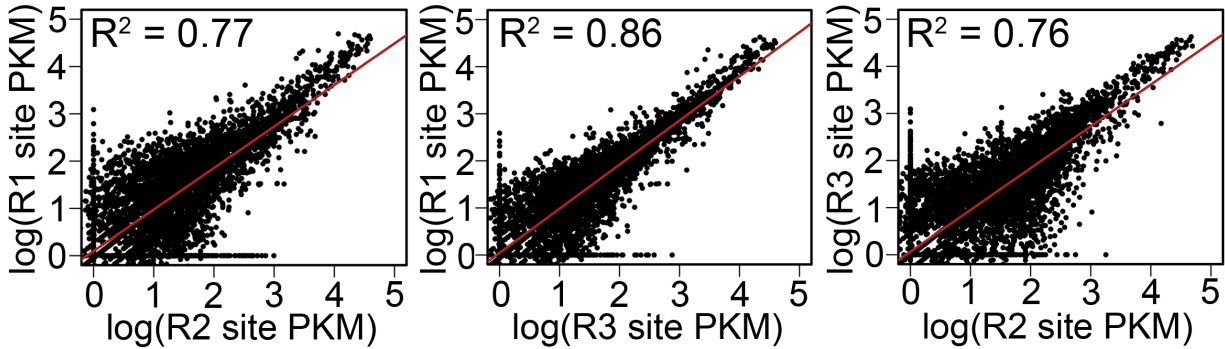


1 **Supplemental Figures**



Pearson correlation coefficient between replicates			
	Dbp2-1	Dbp2-2	Dbp2-3
Dbp2-1	1.00	0.88	0.93
Dbp2-2	0.88	1.00	0.87
Dbp2-3	0.93	0.87	1.00

2

3 **Figure S1. Assessment of reproducibility of Dbp2-binding sites as determined by**

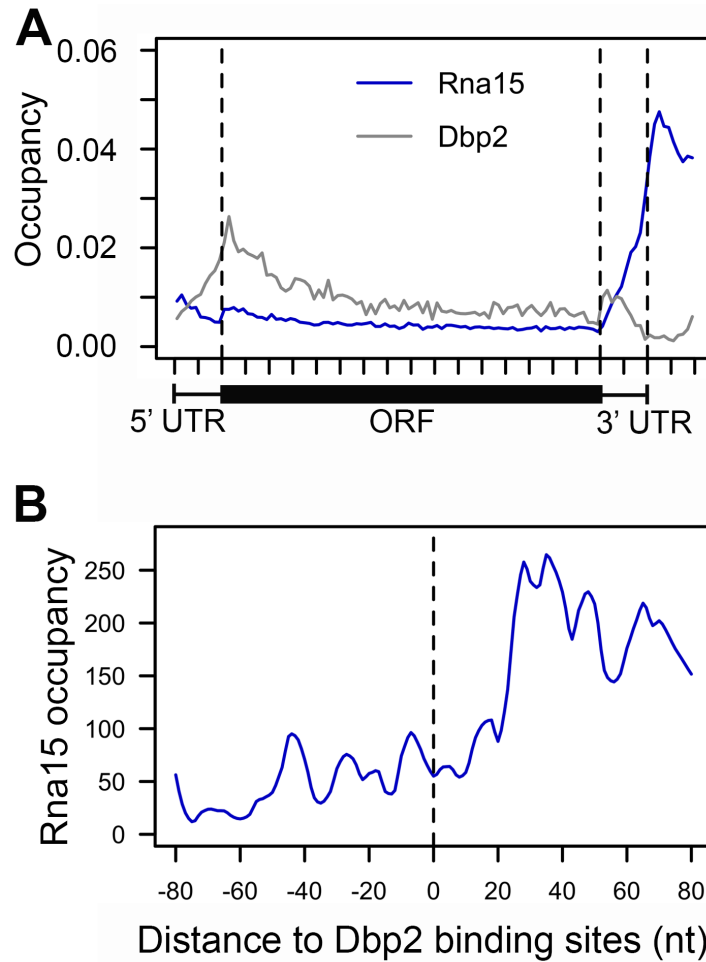
4 **iCLIP-seq across three biological replicates (R1, R2, and R3).** For each replicate,

5 the crosslinking count per kilobase of transcript per million mapped reads (PKM) was

6 calculated. Reproducibility was assessed by calculating Pearson's correlation coefficient

7 between each pair of replicates (table below).

8



10

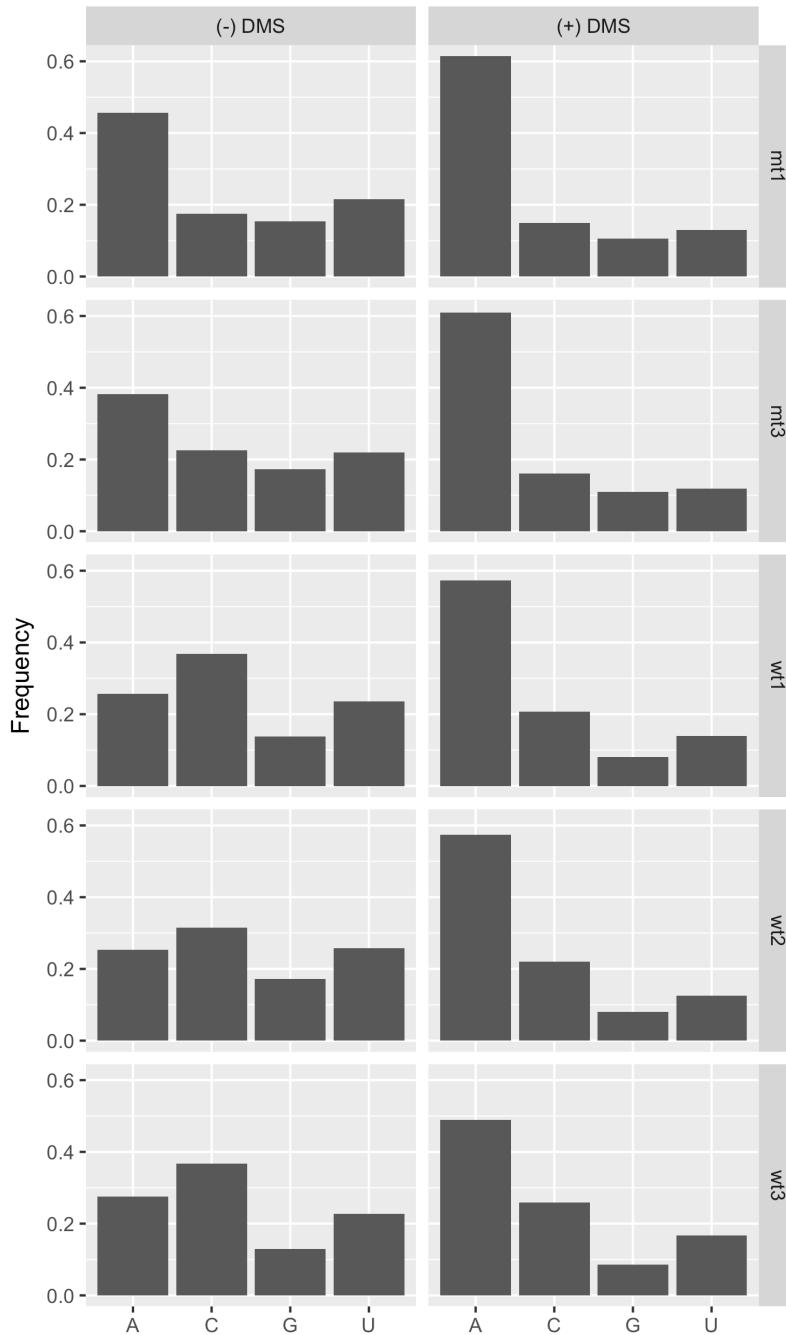
11 **Figure S2. Dbp2 binding at the 3' ends of protein-coding transcripts does not**
 12 **correlate with Rna15 component of the cleavage and polyadenylation complex**

13 **(CPF).** (A) Meta-analysis of Dbp2 (grey) and Rna15 (blue) RNA-binding sites across all

14 commonly bound mRNAs (Rna15 sites from (Baejen et al., 2014)). (B) The distance

15 between Dbp2 and Rna15 binding sites in all commonly bound mRNAs.

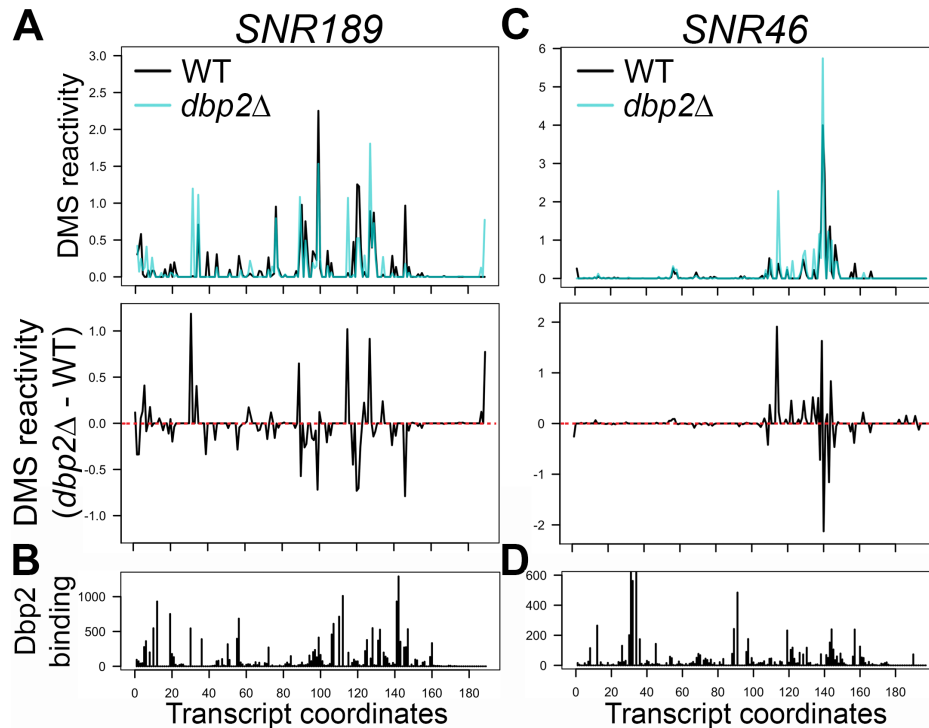
16



17

18 **Figure S3. The frequency of RT stops at A, U, C, and G in each replicate of DMS-**
 19 **treated (+) and untreated (-) samples.** Vertical strip labels indicate strain ('mt' for
 20 *dbp2Δ* and 'wt' for wild type) and replicate batch number. Note reactivity bias towards A,
 21 consistent with prior studies (Ding et al., 2014; Rouskin et al., 2013).

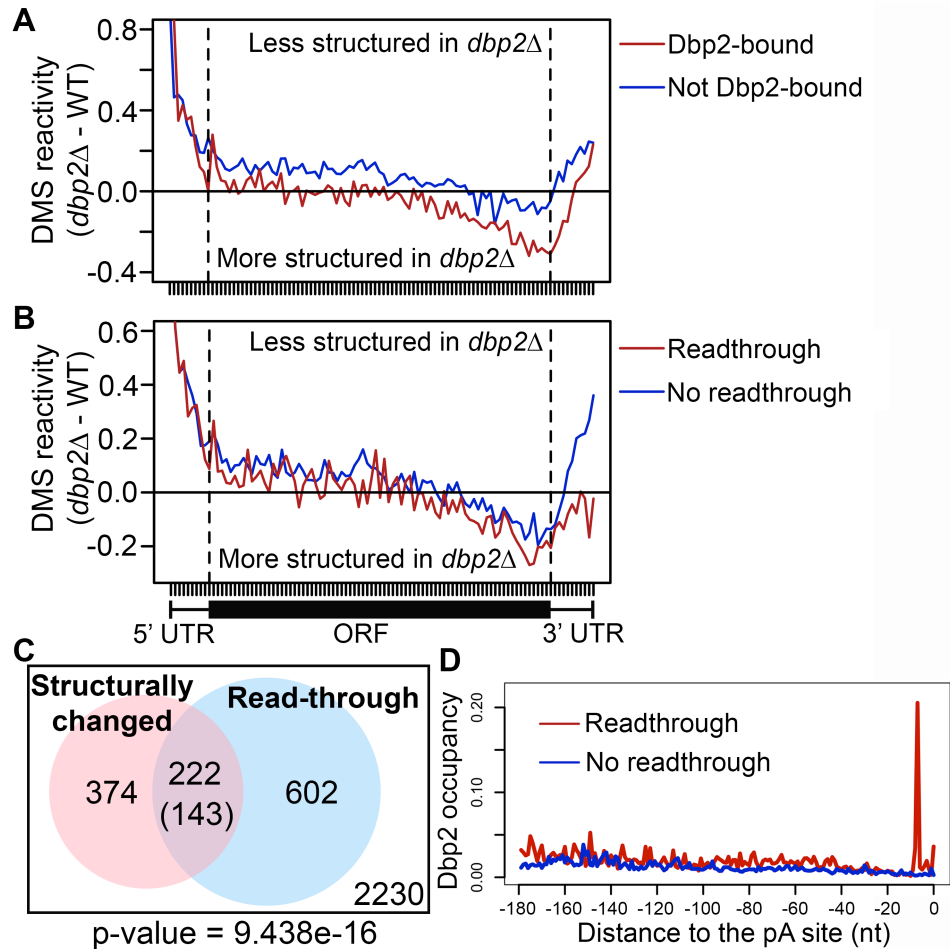
22



24

25 **Figure S4. DMS reactivity (A, C) and Dbp2 binding (B, D) profiles of the two**
 26 **snoRNAs with a read-through defect in *dbp2Δ*.** The reactivity towards DMS for each
 27 nucleotide was normalized using 2-8% approach in each replicate, and the value shown
 28 on the Y-axis is the average from biological replicates of the same strain (i.e. wild type
 29 or *dbp2Δ*). The numbers at the X-axis represent the transcript coordinates relative to the
 30 start of mature 5' end, and the end position on the X-axis corresponds to the mature 3'
 31 end. *DBP2*-dependent changes in DMS reactivity are also presented as the values
 32 derived by subtracting the reactivity in wild type from the reactivity in *dbp2Δ* (A, bottom).
 33 Note that SNR189 also exhibits Dbp2-dependent processing as evidenced by non-
 34 templated A's in *dbp2Δ* (Figure 1E).

35



37

38 **Figure S5. The presence of *DBP2*-dependent structural changes in 3' UTRs**

39 **correlates with a requirement for *DBP2* in transcriptional termination. (A)**

40 Metagene analysis of *DBP2*-dependent changes on secondary structure in transcripts

41 bound (red) or not bound (blue) by Dbp2. *DBP2*-dependent structural changes were

42 captured by the differential reactivity of DMS in $dbp2\Delta$ versus wild type cells. (B)

43 Metagene analysis of *DBP2*-dependent DMS reactivity changes as plotted with respect

44 to the presence (red) or absence (blue) of a read-through defect in $dbp2\Delta$. (C) A Venn

45 diagram showing the intersection between transcripts with read-through defects and

46 those with significant structural changes in $dbp2\Delta$ (determined using dStruct described

47 in methods). The number in the parentheses is the expected value of intersection if the
48 two groups of transcripts have no significant relationship. The p-value derived from a
49 one-sided Fisher's exact test is shown below the box. The number shown in the square
50 corresponds to transcripts without a read-through defect and a statistically significant,
51 structural change in *dbp2Δ*. In this analysis, only transcripts that were passed to the
52 read-through and DMS reactivity analyses are included. (D) Meta-analysis of Dbp2
53 binding within 200 nt upstream of annotated polyadenylation sites of mRNAs with (red)
54 or without 3' extension (blue) upon *DBP2* deletion.
55

56 **Supplementary Tables (Table S1 and S3 are in separate excel files)**
57

58 **Table S1. The list of read-through transcripts in *dbp2*Δ. The ratio of 3' extended /**
59 **total transcripts is also listed for both wild type and *dbp2*Δ.**

60

61 **Table S2. The contingency table for a Fisher's exact test of the correlation**
62 **between the list of transcripts bound by Dbp2 at the 3' end and transcripts with**
63 **read-through defects in *dbp2*Δ (related to Figure 3)**

		Read-through in <i>dbp2</i> Δ		
		Yes	No	Total
Dbp2-bound at 3' end	Yes	222	497	719
	No	602	2107	2709
	Total	824	2604	3428

64

65 **Table S3. The list of transcripts with significant *DBP2*-dependent structural**
66 **changes.**

67

68 **Table S4. The contingency table for a Fisher's exact test of the correlation**
69 **between the list of Dbp2-bound transcripts and transcripts with significant *DBP2*-**
70 **dependent structural changes**

		Significant <i>DBP2</i> -dependent structural changes		
		Yes	No	Total
Dbp2- bound	Yes	468	1107	1575
	No	144	2962	3106
	Total	612	4069	4681

71

72

73

74

75

76 **Table S5. The contingency table for a Fisher's exact test of the correlation**
 77 **between the list of transcripts with read-through defects in *dbp2* Δ and transcripts**
 78 **with significant *DBP2*-dependent structural changes (related to Figure S5)**

		Significant <i>DBP2</i> -dependent structural changes		
		Yes	No	Total
Read-through in <i>dbp2</i> Δ	Yes	180	644	824
	No	321	2283	2604
	Total	501	2927	3428

79
80